Heat Transfer Enhancement of the Film Flow Falling along Vertical Fluted Plates

Shouta Satou and Takahiro Adachi
Department of Mechanical Engineering, Akita University, Tegata-gakuen1-1, Akita, 010-8502, Japan

Keywords: Liquid Film Flow, Heat Transfer, Graetz-Nusselt's Problem, CLSVOF, GFM.

Abstract: Heat transfer enhancement of the film flow falling along vertical rectangular fluted plates is investigated in this study. We have calculated the temporal evolution of the film flow by using the CLSVOF and GF methods, and obtained the steady state film and velocity distributions. It is found that the film flow goes inside the fluted part due to the effect of the surface tension for the fluted plate and the thickness near the fluted edge is thinner. This may lead to the heat transfer enhancement. Therefore, the temperature distribution is calculated in the thermally inlet region, which corresponds to the problem of two-phase version of the well-known Graetz-Nusselt's problem. Finally, we show the relation among the heat transfer, fluted geometries and the surface tension effect.

1 INTRODUCTION

Absorption refrigeration systems have taken an increasing interest due to the global warming problem. The systems are regarded not only as environmentally friendly alternatives to the fluorocarbon-based systems, but also as energy efficient heating and cooling technology (Berlitz et al., 1999). An absorber is a major component in the absorption refrigeration systems because it greatly affects the overall system performance. There are two types of absorbers. One is a plate-type absorber, while the other is a tube-type one. Generally, the plate-type absorber is superior to the tube-type one from the point of view of lightness, compactness, maintenance, etc. under the same operating conditions. Therefore we focus our attention on the plate-type absorber in this study.

In the plate-type absorber, a thin liquid film flow is observed and plays an important role in heat and mass transfer. Therefore, the characteristics of the thin falling liquid film along a vertical flat plate and the corresponding temperature characteristics have been extensively investigated both experimentally and numerically (Kapitza and Kapitza, 1965, Kranz and Goren, 1971, Pierson and Whitaker, 1977).

Recently, increasing the demand for smaller space and lower noise level tends to make representative size and velocity smaller. Therefore, it is important to enhance the heat transfer in the laminar flow regime. In order to enhance the heat transfer, rectangular, triangular or sinusoidal fluted parts along the stream-wise direction have been established on the plate. This is because the liquid film spreads as thinly as possible over the plate surface since strong surface tension aids in the removal of film from the top to bottom of the fluted parts, thereby producing a very thin liquid film. This is called a drainage effect (Gregorig, 1954, Kedzierski and Webb, 1990).

However, it is difficult to clarify the detailed mechanism of the heat transfer enhancement, because the film flow has thin, three-dimensional and unsteady behaviour. Actually, it has been shown that the film flow on the flat plate behaved like a wave and thickness of the film flow became thinner locally in the wavy flow regime, which leads to the enhance of the heat transfer enhancement (Miyara, 2000, 2001, Al-Sibai, 2002). In case of the fluted plate, the situation must be more complicated. So, it is greatly depends on numerical calculations to clarify the flow and temperature characteristics.

In this study, we numerically investigate the thin liquid film flow on the vertical rectangular fluted plates in laminar flow resume. Our objective is to clarify effects of grooved geometries and surface tension on both the flow patterns and the heat transfer by setting the fluted parts on the vertical flat plate. Then, we treat our study under the well-known

Satou S. and Adachi T..
Heat Transfer Enhancement of the Film Flow Falling along Vertical Fluted Plates.
DOI: 10.5220/0005104306070612
In *Proceedings of the 4th International Conference on Simulation and Modeling Methodologies, Technologies and Applications* (SIMULTECH-2014), pages 607-612
ISBN: 978-989-758-038-3

Graetz-Nusselt's problem. This means that the film flow is three-dimensional and fully developed in the stream-wise direction, while the temperature is developing in the thermally inlet region. We will try to show the relation among the heat transfer, fluted geometries and the surface tension effect.

2 MATHEMATICAL FORMULATION

2.1 Mathematical Model

We consider a two-phase flow along a fluted plate as shown in Fig.1 (a). We take a half of groove which is enclosed by broken lines in Fig.1 (a). Figure 1 (b) depicts the plate cross section taken from Fig.1 (a) and indicates the geometric quantities that define its shape. The plate consists of smooth part of width w_l^*, fluted part of width w_b^* and height d^* measured from the bottom of the groove, which is symmetric with respect to the broken lines in Fig.1 (b). We pay attention only to the typical cross-section shown in Fig.1 (b) by considering symmetric condition.

2.2 Governing Equations

The flow is assumed to be three-dimensional, incompressible and fully developed steady state. In addition, a velocity is assumed to be unchanged in *z* direction. It is impossible to find the liquid film flow distribution along the fluted plate surface at steady state in advance, so we calculate the unsteady momentum equations in *x* and *y* directions. Next, we calculate the momentum equations in *z* direction under the steady condition due to fully developed flow. After that, the film flow distribution is calculated by using the velocity profiles. Finally, the energy equation in the thermally inlet region is solved. This is recognized as a problem of two-phase version of the well-known Graetz-Nusselt's problem.

The governing equations for the velocity and pressure are written in non-dimensional forms as

$$\frac{\partial u}{\partial x}+\frac{\partial v}{\partial y}=0\,, \tag{1}$$

$$\rho\left(\frac{\partial u}{\partial t}+u\frac{\partial u}{\partial x}+v\frac{\partial u}{\partial y}\right)= \frac{1}{Re}\left\{\frac{\partial}{\partial x}\left(2\mu\frac{\partial u}{\partial x}\right)+\frac{\partial}{\partial y}\left(\mu\frac{\partial v}{\partial x}+\mu\frac{\partial u}{\partial y}\right)\right\}-\frac{\partial p}{\partial x}, \tag{2}$$

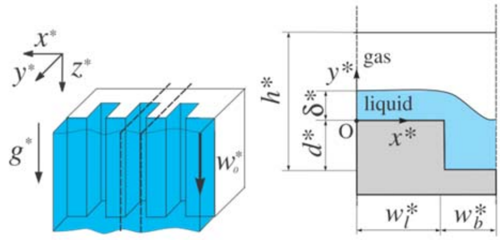

(a) (b)

Figure 1: Physical model and coordinates.

$$\rho\left(\frac{\partial v}{\partial t}+u\frac{\partial v}{\partial x}+v\frac{\partial v}{\partial y}\right)= \frac{1}{Re}\left\{\frac{\partial}{\partial x}\left(\mu\frac{\partial v}{\partial x}+\mu\frac{\partial u}{\partial y}\right)+\frac{\partial}{\partial y}\left(2\mu\frac{\partial v}{\partial y}\right)\right\}-\frac{\partial p}{\partial y}, \tag{3}$$

$$\rho\left(u\frac{\partial w}{\partial x}+v\frac{\partial w}{\partial y}\right)= \frac{1}{Re}\left\{\frac{\partial}{\partial x}\left(\mu\frac{\partial w}{\partial x}\right)+\frac{\partial}{\partial y}\left(\mu\frac{\partial w}{\partial y}\right)\right\}+\rho Fr-\frac{\partial p}{\partial z} \tag{4}$$

where velocity gradient in *z* direction is ignored such as $\partial u/\partial z=\partial v/\partial z=\partial w/\partial z=0$ in the equations (1), (2), (3) and (4) because of assumption as velocity **u** is unchanged in *z* direction.

The governing equations for the temperature is written in non-dimensional forms as

$$\rho c_p\left(u\frac{\partial T}{\partial x}+v\frac{\partial T}{\partial y}+w\frac{\partial T}{\partial z}\right) =\frac{1}{PrRe}\left\{\frac{\partial}{\partial x}\left(\lambda\frac{\partial T}{\partial x}\right)+\frac{\partial}{\partial y}\left(\lambda\frac{\partial T}{\partial y}\right)\right\} \tag{5}$$

where heat conduction term in *z* direction is omitted in the equation (5) because heat conduction in *z* direction is smaller than one in *x* and *y* directions.

All the variables have been non-dimensionalized using a characteristic length δ^*, a film surface velocity w_0^*, the density of the liquid phase ρ_l^*, the temperature on the plate T_w^* and the temperature in gas phase T_s^* as

$$x=\frac{x^*}{\delta^*},y=\frac{y^*}{\delta^*},z=\frac{z^*}{\delta^*},\quad u=\frac{u^*}{w_0^*},v=\frac{v^*}{w_0^*},w=\frac{w^*}{w_0^*},\quad t=\frac{t^*w_0^*}{\delta^*},p=\frac{p^*}{p_l^*{w_0^*}^2},T=\frac{T^*-T_w^*}{T_s^*-T_w^*} \tag{6}$$

where we represent physical quantities with their dimensions by attaching a superscript * to them.

We consider that the density, viscosity, thermal conductivity and specific heat change discontinuously across the interface between the liquid and gas phases and are written as

$$f=\tilde{f}+\left(1-\tilde{f}\right)H\,, \tag{7}$$

where H is the discontinuous step function (Heaviside function) defined as

$$H(\phi) = \begin{cases} 0, & \phi \le 0 \\ 1, & \phi > 0 \end{cases} \quad (8)$$

where ϕ is the level-set function which is defined as a distance function between the center point of calculation cell and gas-liquid interface. In addition, the density, viscosity, thermal conductivity and specific heat are non-dimensionalized based on the values of liquid phase, and they are unity in the liquid phase, defined as follows in the gas phase

$$\tilde{\rho} = \frac{{\rho_v}^*}{{\rho_l}^*}, \tilde{\mu} = \frac{{\mu_v}^*}{{\mu_l}^*}, \tilde{\lambda} = \frac{{\lambda_v}^*}{{\lambda_l}^*}, \tilde{c_p} = \frac{{c_{p_v}}^*}{{c_{p_l}}^*} \quad (9)$$

where subscript l is physical properties in liquid phase and v is physical properties in gas phase.

Non-dimensional geometric parameters are defined as

$$w_l = \frac{w_l^*}{\delta^*}, w_b = \frac{w_b^*}{\delta^*}, d = \frac{d^*}{\delta^*}. \quad (10)$$

Non-dimensional parameters in equations are Reynolds number Re and Prandtl number Pr, defined as

$$Re = \frac{w_0^* \delta^*}{\nu_l^*}, Pr = \frac{\nu_l^*}{\alpha_l^*} \quad (11)$$

where ν_l* is kinematic viscosity of the liquid phase and α_l* the temperature conductivity.

Because there is a special relation between Froude number and Reynolds number(Adachi, 2013), the Froude number is defined as

$$Fr = \frac{1}{Re}\left(\frac{2}{1-\tilde{\rho}}\right)\frac{(h-1)^2 + \tilde{\mu}(2h-1)}{(h-1)^2} \quad (12)$$

where $h = h^*/\delta^*$ is the computational domain in y direction as shown in Fig. 1(b) and h=4 in this study.

2.3 Boundary Conditions

The conservation equations (1)-(4) for each phase are coupled through the discontinuous jump conditions at the interface written in non-dimensional forms as

$$\boldsymbol{u}_l - \boldsymbol{u}_v = 0, \quad (13a)$$

$$-p_l + p_v + \mathbf{n} \cdot \frac{1}{Re}[(\nabla\mathbf{u} + \nabla\mathbf{u}^{\mathrm{T}})_l - \tilde{\mu}_v(\nabla\mathbf{u} + \nabla\mathbf{u}^{\mathrm{T}})_v] \cdot \mathbf{n} = \frac{Fr}{Bo}\kappa \quad (13b)$$

where κ is a curvature of the film surface, $\mathbf{n}$ is an unit normal vector at the interface from the gas phase to the liquid phase and Bo is bond number defined as

$$Bo = \frac{\rho_l^* \delta^{*2} g^*}{\sigma_l^*} \quad (13c)$$

where σ_l* is the surface tension coefficient and g* is the gravitational acceleration. It should be noted that the temperature is assumed to be constant in the gas phase because it plays a model of mass transfer in the gas phase simultaneously. So, the temperature is a saturation constant and unity in the gas phase.

The boundary conditions on the plate surface are given by

$$u = 0, v = 0, w = 0, T = 0. \quad (14)$$

In addition, the flow is assumed to be symmetric along the broken lines indicated in Fig.1 (b). Then the symmetry conditions are expressed as

$$u = \frac{\partial v}{\partial x} = \frac{\partial w}{\partial x} = \frac{\partial T}{\partial x} = 0. \quad (15)$$

Finally, the Sommerfeld radiation condition is imposed at the boundary of the computational domain at y=h as

$$\frac{\partial \boldsymbol{u}}{\partial t} + U\frac{\partial \boldsymbol{u}}{\partial y} = 0 \quad (16)$$

where U is a advection velocity adopted as U=1 in this study.

3 NUMERICAL METHOD

In order to calculate the fully developed film flow, we calculate the velocity **u** by solving equations (1)-(3) under the boundary condition given by equations (13)-(16). Then we use Highly Simplified Marker and Cell (HSMAC) method and Ghost Fluid (GF) method (Kang et al., 2000 and Gibou et al., 2002). HSMAC method is used to be able to calculate velocity and pressure avoiding the calculation of Poisson equation and GF method is used to obtain sharp changes of some physical quantities across the interface between the liquid and gas phases, where a semi-implicit method is used for the calculation of the viscous term (Li et al., 1998).

In addition, we use a Coupled Level Set and Volume of Fluid (CLSVOF) method (Son and Dhir 2007 and Wang et al., 2009) to determine the gas-liquid interface. This method can preserve mass convection and accurately calculate unit normal vector at the interface by using a fluid fraction F and level set function ϕ. The fluid fraction F is defined as a ratio of volume of liquid phase in a cell such as F=1 for the cell filled with liquid phase, F=0 for the cell filled with gas phase and $0<F<1$ for gas-liquid interface, while the level set function ϕ is defined as a distance function between gas-liquid interface and center of the cell.

The pressure gradient in Eq. (4) must be constant because the flow field is fully developed in z direction. The velocity component w is calculated iteratively by using the obtained u, v and p and by changing the value of the constant pressure gradient until satisfying the condition that the flow rate in z direction converges to the corresponding quantity for the flat plate without groove. It should be noted that the flow rate is defined as an integration of the velocity w over the liquid film distribution.

Finally, the energy equation (5) is solved in the thermally inlet region by using the steady velocity field. The temperature is steady but develops in z direction. Therefore, the derivative of temperature with respect to z is discretized with the first order forward differencing. The semi-implicit method is also used for the calculation of the diffusion term.

4 RESULTS

Numerical calculations are carried out for the geometric parameters as follows.

$$w_b = 2, w_l = 3, d = 0, 1, 3, 5 \tag{17}$$

where four different values of height d are used in order to examine an influence of groove on the liquid film flow distribution. Also the other non-dimensional parameters are as follows.

$$\begin{gathered} Re = 50, Pr = 2, Bo = 1, 10, 100, \\ \tilde{\rho} = 0.001, \tilde{\mu} = 0.05, \tilde{\lambda} = 0.0456, \tilde{c_p} = 0.1 \end{gathered} \tag{18}$$

where three different values of Bond number are used in order to examine an influence of surface tension on the liquid film flow distribution. The calculation have been performed by using $\Delta x = \Delta y = 5 \times 10^{-2}$ and $\Delta t = 10^{-5}$.

4.1 Shape of the Liquid Film Flow at Steady State

In order to examine an effect of wettability at the plate surface, we calculate for two different contact angles such as θ=60° and 90°. We show the film and velocity distributions of the fully developed flow at Bo=1, 10 and 100 in Fig.2 for θ=60° and 90°, respectively. In all cases, the distribution of the liquid film becomes thinner at the groove edge as seen in Fig.2. It should be emphasized that a break of the liquid film occurs at the groove edge when the Bond number decreases which corresponds to an increase of surface tension. Namely, removal of the film from the top to bottom decreases due to the break when the surface tension increases. Therefore the drainage effect becomes weaker for the stronger surface tension. Furthermore, we can see the difference for the two different contact angles especially for the break part shown in Fig.2 (a) and (b). The liquid film for 60° is much more pulled into the bottom and the break region becomes larger compared with the case of 90°. This is because the film flow for 60° is more hydrophilic compared with the one for 90°. Therefore, the film distribution after the break depends on the contact angle.

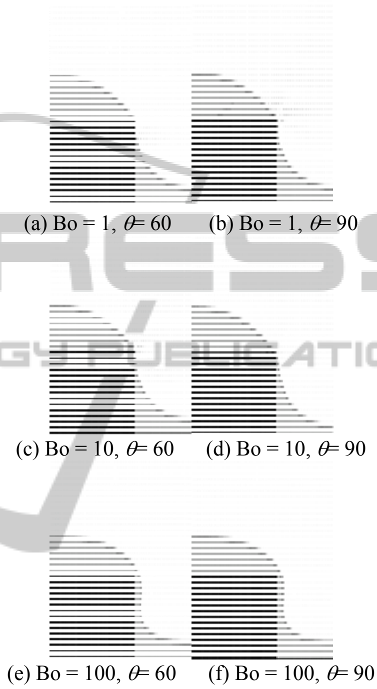

Figure 2: Steady film flow for various Bond numbers and contact angles for d=3.

4.2 Heat Transfer

We consider an effect of groove on the heat transfer from the plate to the gas phase through the film flow. A local Nusselt number Nu is defined as

$$Nu = \frac{\alpha^* \delta_0^*}{\lambda^*} \tag{20}$$

where α^* is the heat transfer coefficient. A local heat flux q^* is defined as

$$q^* = -\lambda^* \frac{\partial T^*}{\partial \mathbf{n}^*} = \alpha^* (T_w^* - T_s^*) \tag{21}$$

where $(\partial T^* / \partial \mathbf{n}^*)$ is the normal temperature gradient to the wall along the plate surface including the groove surface. By introducing equation (21) into equation (20), we can obtain

$$Nu = \frac{-\lambda^* \delta_0^*}{\lambda^* (T_s^* - T_w^*)} \frac{\partial T^*}{\partial n^*} = -\frac{\partial T}{\partial n} \tag{22}$$

where n is a normal direction to the wall and has a positive value from the liquid phase to the plate wall. It should be noted that the local Nusselt number of the flat plate is Nu=1. In addition, we define length s along the wall including groove surface, where the start point of s is origin O.

We take the fully developed case of Bo = 10, d=3 and θ=60° shown in Fig.2 (c) as a typical example of heat transfer and depict the corresponding local Nusselt number distribution in Fig.3. As seen in Fig.2 (c), since the thickness of the liquid film is decreasing toward the groove edge, the local Nusselt number in Fig.3 slowly increases along the flat surface region ($s < 3$). It has a local maximum at the groove edge (s~3). On the other hand, the local Nusselt number suddenly decreases to nearly zero due to the effect of the break of the film flow(s~3). After that, it suddenly increases to a local maximum value and decreases to zero again ($3< s < 6$). It is almost zero at the bottom edge of groove (s=6) because thickness of liquid film flow is too thick to transport the heat to the wall normal direction. It slowly increases again along the surface of groove ($6 < s \leq 8$) due to decrease of thickness of liquid film.

Finally we define a mean Nusselt number Nu_m to investigate an overall heat transfer performance as

$$Nu_m = \frac{1}{w_l + w_b}\int_s Nu\, ds. \tag{23}$$

If the film distribution is corresponding to the Nusselt's solutions along the flat plate, the mean Nusselt number is as Nu_m=1. On the other hand, the mean Nusselt number for the case of Fig.2 (c) is Nu_m= 4.071. It is found that the value of Nu_m is larger than 1. It should be noted that the increase of the heat transfer area for d=3, defined as $(w_l+d+w_b)/(w_l+w_b)$, is 1.6 compared with the flat plate. Therefore, the heat transfer performance for the fluted plate is larger than the increase of the heat transfer area and that of the flat plate in this case.

In addition, we show the results for the other values of d and Bond number in Fig.4. This figure shows the relation between heat transfer, fluted geometries and surface tension. The mean Nusselt number is nearly unity for d=1 because the height d is small and the liquid film covers completely the fluted part so as to cancel the groove effect. When the Bond number decreases, the mean Nusselt number for d=3 slowly increases due to the effect of decrease of film thickness at the side of groove, while it decreases for the smaller Bond number. This is because the break of the film flow proceeds at groove edge as previously mentioned. On the other hand, the mean Nusselt number for d=5 gradually increases even for the smaller Bond numbers, where any break does not occur yet.

5 CONCLUSIONS

A numerical investigation has been performed for the two-phase film flow falling down along fluted plates. Numerical simulations of three-dimensional flow field have been carried out by using the HSMAC method, GF method and the CLSVOF methods based on the finite difference methods for the plate configuration $w_l = 3, w_b = 2, d = 1,3,5$ and for the non-dimentional parameters $Re = 50$, $Pr = 2$, and $Bo = 1,\ 10,\ 100$.

It is found that the thickness of the film flow becomes thinner than that of the flat plate because the film flow falls down into fluted part removing the film from the top to bottom. However, the break of the liquid film occurs at the groove edge which restricts the removal of the film. Heat transfer is enhanced for the film flow falling down along the fluted plate, because the liquid film becomes thinner. Once the break of the film occurs, however, the heat transfer across the liquid film disappears. So, the mean Nusselt number decreases for the film flow with the break even if the averaged film thickness is thin.

It should be noted that the film flow falling under the influence of gravity ceases to be laminar and constant in the stream-wise direction when the flow rate is increased. Waves tend to appear on the free surface, and the flow becomes turbulent as the flow rate is further increased. It is our future work to investigate such unsteady flow and temperature fields in the fluted plates.

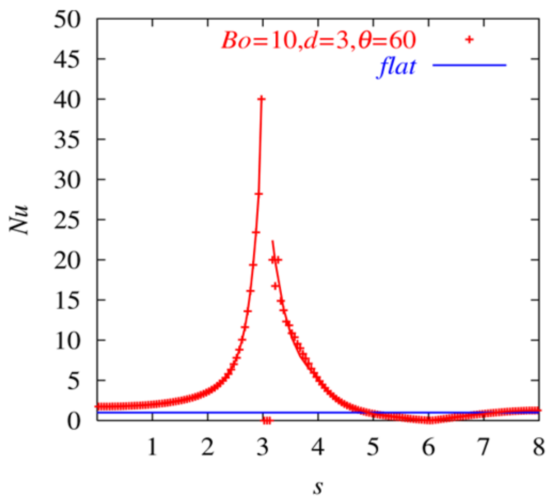

Figure 3: Local Nusselt number along fluted plate.

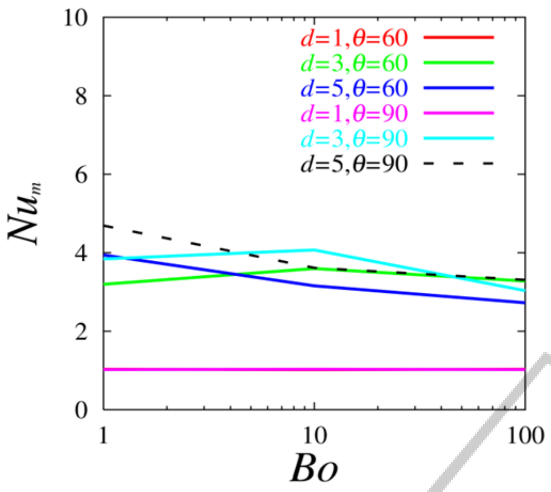

Figure 4: Mean Nusselt number for difference parameters.

ACKNOWLEDGMENTS

The computation in this study has been done using the facilities of the Supercomputer Centre, the Institute of Statistical Mathematics (H24-T-25).

REFERENCE

Berlitza, T., Satzgera, P., Summererb, F., Zieglera, F. and Alefeldb, G. 1999. A contribution to the evaluation of the economic perspectives of absorption chillers, *International Journal of Refrigeration,* Vol. 220, pp.67-76.

Kapitza, P., L. and Kapitza, S., P., 1965. Wave flow of thin layers of viscous fluid, *Colleted papers of P.L. Kapitza* (Edited by D. T. Haar), Vol. 2, Pergamon Press, Oxford, pp.662-709.

Krantz, W., B. and Goren, S., L., 1971. Stability of thin liquid films flowing down a plate, *Ind. Eng. Chem. Fundam*., Vol. 10, pp.91-101.

Pierson, F., W. and Whitaker, S., 1977. Some theoretical and experimental observations of the wave structure of falling liquid films, *Ind. Eng. Chem. Fundam*., Vol. 16, pp.401-408.

Gregorig, R., 1954. Hautkondensation an feingewellten oberflaechen bei beruchsichtigung der oberflaechenspannungen, *Z. Angew. Math. Phys*., Vol. 5, pp.36-49.

Kedzierski, M., A. and Webb, R., L., 1990. Practical fin shapes for surface-tension-drained condensation, *ASME J. Heat Trans*., Vol. 112, pp.479-485.

Miyara, A., 2000. Numerical simulation of wavy liquid film flowing down on a vertical wall and an inclined wall. *Int. J. Therm. Sci*., Vol. 39, pp.1015-1027.

Miyara, A., 2001. Flow dynamics and heat transfer of wavy condensate film. *Transactions of the ASME J. Heat Transf.*, Vol. 123, pp.492-500.

Al-Sibai F, Leefken, A. and Renz, U., 2002. Local and instantaneous distribution of heat transfer rates through wavy films, *Int. J. Therm. Sci.*, Vol. 41, pp.658-663.

Li, J., Renardy, Y., Y. and Renardy, M., 1998. A numerical study of periodic disturbance on two-layer coquette flow, *Physics of Fluids,* Vol.10, number 12, pp.3056-3071.

Kang, M., Fedkiw, R., P. and Liu, X-D., 2000. A boundary condition capturing method for multiphase incompressible flow, *J. Sci. Comput.,* Vol.15, pp.323-360.

Gibou, F., Fredkiw, R., P., Cheng, L-T. and Kang, M., 2002. A second-order-accurate symmetric discretization of the poisson equation on irregular domains, *Journal of Computational Physics,* Vol.176, pp.205-227.

Son, G. and Dhir, V., K., 2007. A level set method for analysis of film boiling on an immersed solid surface, *Numerical Heat Transfer, Part* B, Vol.52, pp.153-177.

Wang, Z., Yang, J., Koo., B. and Stern, F., 2009. A coupled level-set and volume-of-fluid method for sharp interface simulation of plunging breaking waves, *Int. J. Multiphase flow*, Vol.35, pp.227-246.

Adachi, T., 2013. Velocity and temperature profiles extending over the liquid and gas phases of two-phase flow falling down vertical plates, *Applied Thermal Engineering,* Vol.51, pp.827-832.